



## Removal of organic pollutants and recovery of crystalline salt from ammonium sulfate waste salt by antisolvent crystallization process

Xinyu Huang <sup>a,b,c</sup>, Hao Wang <sup>a,b,c</sup>, Sajun Lv <sup>d</sup>, Haoqing Zhang <sup>a,b,c</sup>, Chuqi Wang <sup>a,b,c</sup>,  
Xiuxiu Ruan <sup>a,b,c,\*</sup>

<sup>a</sup> School of Environmental and Chemical Engineering, Shanghai University, No. 99 Shangda Road, Shanghai, 200444, China

<sup>b</sup> Key Laboratory of Organic Compound Pollution Control Engineering(MOE), School of Environmental and Chemical Engineering, Shanghai University, Shanghai, 200444, China

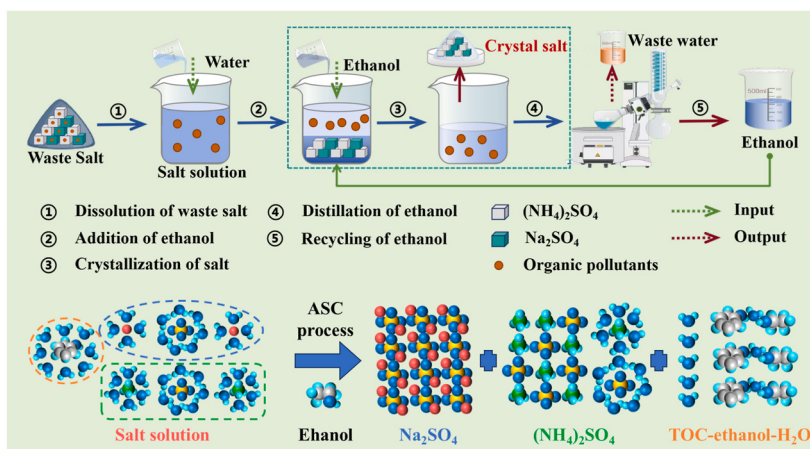
<sup>c</sup> Center of green Urban Mining & Industry Ecology, Shanghai University, No.99 Shangda Road, Shanghai, 200444, China

<sup>d</sup> Shaoxing Shangyu Zhonglian Environmental Protection Co., Ltd., Zhejiang, 312300, China

### HIGHLIGHTS

- ASC efficiently removes organic pollutants and recovers crystalline salt from ammonium sulfate waste salt.
- Ethanol can be recycled 7 times with 93.99 % TOC removal efficiency maintained.
- ASC outperforms pyrolysis and advanced oxidation in TOC removal.
- Ethanol disrupts salt ion solvation shell, promoting recrystallization and releasing organics.

### GRAPHICAL ABSTRACT



### ARTICLE INFO

**Keywords:**  
Waste ammonium salt  
Ammonium sulfate  
Organic pollutants  
Antisolvent crystallization  
Recycling

### ABSTRACT

The main challenge of industrial waste ammonium salt recycling is the efficient removal of organic pollutants. Conventional pyrolysis process cannot be used due to ammonium salts readily decompose at temperatures well below typical pyrolysis ranges, resulting in nitrogen loss and product alteration. To address this, an efficient antisolvent crystallization (ASC) method is developed for simultaneous organic pollutant removal and salt recovery. The results show that ethanol, as an efficient antisolvent, can achieve a total organic carbon (TOC) removal rate of approximately 96.44 % and a salt recovery rate of 85.07 % when used in a 2:1 vol ratio with the waste salt solution. The optimal operating conditions are a temperature range of 0–30 °C, a pH range of 2–8, and a reaction time of 60 min. Ethanol can be effectively recycled and reused for over seven times while maintaining approximately 93.99 % TOC removal efficiency. Elemental mapping of the waste salt after treatment shows a

\* Corresponding author. School of Environmental and Chemical Engineering, Shanghai University, No. 99 Shangda Road, Shanghai, 200444, China.  
E-mail address: [ruanxiuxiu@shu.edu.cn](mailto:ruanxiuxiu@shu.edu.cn) (X. Ruan).

carbon content as low as 0.3 %, indicating efficient removal of organic pollutants. Compared to the maximum TOC removal rates achieved by pyrolysis(87.43 %) and advanced oxidation(86.17 %) processes, the ASC process demonstrates superior performance with a removal efficiency exceeding 95 % under ambient temperature conditions. Mechanism analysis reveals that adding ethanol to the saturated waste salt solution can induce salt ion recrystallization and release organic pollutants into the solution, thereby achieving efficient separation of salt and organic pollutants. This study provides an environmentally and economically feasible solution for the treatment of ammonium sulfate waste salt.

## 1. Introduction

With the rapid development of modern industrial production, the production of waste salt has increased dramatically, which has become an urgent environmental problem to be solved in the industrial field (Wang et al., 2023). These waste salts, which contain a significant amount of organic pollutants, pose a severe threat to ecosystems and human health, thereby greatly hindering the resource utilization of waste salt (Wang et al., 2021). China's annual production of waste salt exceeds  $2 \times 10^7$  tons, primarily originating from industries such as coal chemical, petrochemical, dyeing, pharmaceutical, and pesticide manufacturing (Ruan et al., 2024). Based on their thermal stability characteristics, waste salts can be categorized into two types. The first type, which exhibits good thermal stability and primarily consists of sodium chloride and sodium sulfate (Annamalai et al., 2022). This type of waste salt has been extensively studied for resource utilization, with pyrolysis technology commonly employed to eliminate organic pollutants (Dong et al., 2024). In contrast, the second type of waste salt, characterized by poor thermal stability and mainly composed of ammonium sulfate or ammonium chloride (Zhang et al., 2019). These are mainly produced in the process such as coal to ammonia production, flue gas desulfurization via ammonia method, pesticide ammoniation, and antibiotic salt crystallization (Zhang et al., 2021; Ni et al., 2019). However, due to the difficulty in removing organic pollutants from waste ammonium salts, their resource recovery technologies have not received enough research attention (Feng et al., 2025). Currently, the primary disposal method for waste ammonium salt is landfill, a practice that not only consumes substantial land resources but may also lead to issues such as groundwater contamination, thereby exerting significant pressure on sustainable environmental development (Yaashikaa et al., 2022).

In the search for organic pollutant removal technologies for waste ammonium salts, the experience of conventional waste salt treatment with good thermal stability has important reference value. Pyrolysis, a mainstream industrial technology, heats waste salts at around 500 °C to decompose organic matter into gases or partially carbonize them into solids, achieving up to 96.32 % organic pollutant removal (Xi et al., 2023). Melt treatment, which heats waste salts to high temperatures of 800–1200 °C, has a universal destructive ability for almost all types of organic pollutants, and the removal rate is stably exceeding 99 % (Lin et al., 2018; Zhao et al., 2023). Nevertheless, during high-temperature pyrolysis, waste ammonium salts with poor thermal stability is easy to decompose, generating corrosive gases like ammonia. This poses potential damage to equipment and reduces the salt product recovery rate (Zelenková and Slovák, 2022). Solvent elution, based on the "like dissolves like" principle, removes organic pollutants by adding organic solvents to waste salts (Wang et al., 2024a). Yet, when applied to waste ammonium salts, this method only achieves a TOC removal rate of 67.57 % (Huang et al., 2024). Additionally, after dissolving waste salts in water to form brine wastewater, advanced oxidation can be used. This method employs highly active oxidants to oxidize and decompose organic pollutants in wastewater, but the actual treatment effect is affected by the high salt environment. For example, the organic removal rate of the Fenton process is only 61 % (Liu et al., 2021). The main reason may be that the inorganic anions contained in the wastewater may weaken or even block the activity of free radicals, thus affecting the

treatment effect (Domingues et al., 2022; Li et al., 2024). Membrane treatment separates pollutants from brine by controlling the osmotic pressure difference across the membrane (Goh et al., 2022). Ultrafiltration membranes, for example, achieve 82.4 % TOC removal from textile wastewater (Ćurić et al., 2021). Nevertheless, when dealing with complex industrial waste salts, there is still a need to develop membrane materials with good permeability and anti-fouling properties (Ahmad et al., 2021). Overall, existing treatment methods generally have problems such as low salt recovery rate (Lu et al., 2025), insufficient technical maturity (Du et al., 2023), and poor TOC removal efficiency (Gholami et al., 2024) when treating waste ammonium salts, which are difficult to meet the needs of efficient treatment and resource utilization. In contrast, the emerging ASC process in recent years has shown potential in effectively treating waste ammonium salts by efficiently removing TOC and recovering crystalline salts (Sahu et al., 2024; Huang et al., 2025). Organic pollutants in wastewater are categorized into water-soluble and non-water-soluble (Wang et al., 2024b). Based on this, this study proposes the following hypothesis: Using the ASC process to treat waste ammonium salts, water-soluble organic pollutants are dissolved in the aqueous phase, while non-water-soluble organic pollutants are dissolved in the organic solvent phase. Combined with the recrystallization process of salt, organic pollutants are effectively separated.

The ASC process removes organic pollutants by forming a salt saturated solution, adding an antisolvent to create an aqueous two-phase system (ATPS), and extracting the pollutants and remove them (Feng et al., 2024). During this process, the salt components recrystallize, allowing for recovery by filtration (Sussens et al., 2024). According to the available literature, the application of ASC to waste salt treatment remains in its infancy, with all existing research have focused on waste sodium salt systems, and research on waste ammonium salts has not been reported. Significant variations in organic pollutant removal efficiency are observed depending on the antisolvent type, such as greater performance of ethanol than acetone due to its lower **polarity** (Lo et al., 2024) and **lower solubility for salts** (Qiu et al., 2020). For instance, when treating waste salts primarily composed of sodium chloride, using ethanol as the antisolvent can achieve a high TOC removal rate of up to 95.4 % (Feng et al., 2024), whereas acetone only yields an 81.96 % TOC removal rate (Li et al., 2020a). Beyond pollutant removal, ASC also demonstrates salt recovery capabilities. Previous studies have shown that salt recovery depends on both solvent miscibility and salt solubility. Methanol, ethanol and dimethyl sulfoxide effectively recover sodium, potassium and magnesium salts, whereas acetone and acetonitrile are selective for potassium salts (Sahu et al., 2024). Sulfate salts experience a sharp solubility drop upon antisolvent addition, enabling yields as high as 95.6 % for sodium sulfate with methanol (Bhatti et al., 2024). In contrast, chloride salts show only modest solubility reduction, exemplified by sodium chloride crystallizing at merely 52.13 % with ethanol (Feng et al., 2024). However, the applicability of ASC for ammonium salt crystallization recovery is not yet clear (Feng et al., 2025). Notably, antisolvent recycling and reuse must be prioritized to reduce operational costs and minimize environmental impacts (Raluy et al., 2006). Antisolvent recycling process for mixed sodium chloride and sodium sulfate salts was found to achieve a cost reduction of 32.13 %, compare to the process without antisolvent recovery process, as well as 3058 kg CO<sub>2</sub> eq. per ton of carbon emssion reduction (Sahu et al., 2024). Therefore, the

systematic screening of efficient antisolvents suitable for waste ammonium salt systems and the optimization of their recycling processes are crucial for advancing the application of ASC technology in this field.

Based on the above research needs, this study aims to develop an ASC treatment strategy for waste ammonium salts by screening efficient antisolvents and optimizing their recycling processes. Using actual ammonium sulfate waste salt was selected as the research object, and the effect of antisolvent on the removal of organic pollutants and the increase of crystal salt yield was systematically analyzed. By exploring the effects of antisolvent type, dosage, temperature, reaction time and pH on the treatment effect, the optimal process parameters of ethanol as antisolvent were determined. The recovery conditions of ethanol were further optimized, and the recycling effect of the recovered solvent was proved. In addition, the mechanism of anti-solvent removal of organic pollutants and the quality characterization of product salt were investigated. This study provides an innovative solution for the resource utilization of waste ammonium salt and promotes the development of industrial waste salt treatment technology.

## 2. Materials and methods

### 2.1. Samples and chemicals

The waste salt was obtained from a dyeing factory. It was recovered by evaporative crystallization of the hypersaline wastewater after the diazotization and coupling stages in the production disperse dyes. The residual organics in the salt were mainly phenol, trichlorobenzene, and xylenes. The waste salt used in this study was obtained from a pharmaceutical company in Shaoxing, Zhejiang Province, China. It was generated by evaporating high-salinity wastewater from the production of pharmaceutical intermediates. As shown in Table S1, the waste salt primarily consists of  $(\text{NH}_4)_2\text{SO}_4$  and  $\text{Na}_2\text{SO}_4$ , with a TOC content of 0.75 %, and is referred to as ammonium sulfate waste salt. When prepared as a saturated solution, it appears as a transparent pale yellow liquid (Fig. S1). All analytical-grade chemicals, including methanol, ethanol, isopropanol, acetonitrile, ethyl acetate, benzene, and toluene, were supplied by Sinopharm Chemical Reagent Co., Ltd. (China). The water used in the experiments had a conductivity ranging from 2.43 to 9.87  $\text{M}\Omega \text{ cm}$  and was deionized.

### 2.2. ASC process for ammonium sulfate waste salt

Fig. 1 illustrated the process of removing organic pollutants from waste salt and recovering crystalline salt using the ASC process. The procedure involved the following steps. First, ammonium sulfate waste salt was mixed with water in proportion and stirred thoroughly in a water bath at 25 °C to obtain a saturated salt solution. Next, a specific amount of ethanol (initial purity 99.5 %) was added to induce inorganic salt ion crystallization. Then, the solid and liquid phases were separated using a vacuum filtration device, and the collected crystals were dried at 70 °C. In the solvent recovery stage, the ethanol-containing solution was introduced into a distillation system. Distillation was stopped when the

distilled liquid volume reached the initial ethanol addition. The recovered ethanol was recycled. The remaining solution containing impurities was treated as wastewater.

### 2.3. Antisolvent screening experiment

Saturated salt solutions of  $(\text{NH}_4)_2\text{SO}_4$  (760 g/L) and  $\text{Na}_2\text{SO}_4$  (280 g/L) were prepared using analytical grade reagents. In the experiment, 10 mL of each salt solution was transferred to a centrifuge tube. Antisolvents were selected according to the difference of polarity and hydrogen bonding ability, different antisolvents (30 mL each)-methanol, ethanol, n-propanol, isopropanol, n-butanol, acetonitrile, acetone, and glacial acetic acid were added to each tube. After addition, the experimental parameters were determined according to the pre-test results. The mixtures were shaken for 120 min to ensure thorough mixing. Then, they were centrifuged at 3000 rpm for 5 min to separate the phases. The crystallized salt was dried in a 70 °C oven for 48 h. Finally, the yield of product salt from each antisolvent was determined by the gravimetric method, and the most suitable antisolvent was identified.

### 2.4. Practical waste salt utilization effects

Saturated solutions were prepared using real ammonium sulfate waste salt. For each experiment, 50 mL of the solution was placed in a conical flask, and 150 mL of the aforementioned eight antisolvents and seven binary solvent mixtures (A: methanol-ethanol, B: methanol-acetone, C: ethanol-acetone, D: methanol-acetonitrile, E: ethanol-acetonitrile, F: methanol-isopropanol, G: ethanol-isopropanol) were added. All binary system were combined at a 1:1 vol ratio, a proportion widely employed in antisolvent crystallization studies (Yang et al., 2019). After stirring and filtering, the product salt yield was determined by drying. The organic removal rate was measured using a total organic carbon analyzer, and the ion composition was analyzed by ion chromatography. Based on the results, methanol and ethanol, which showed better treatment effects, were selected. Their addition volumes (25, 50, 75, 100, 125, and 150 mL) were varied to study their impact. Furthermore, analytical grade reagents were used to simulate waste salt of different concentrations. The mass ratios of  $(\text{NH}_4)_2\text{SO}_4$  to  $\text{Na}_2\text{SO}_4$  were set at 0.25, 0.5, 1, 1.5, 2, 2.5, and 4, and 100 mL of methanol or ethanol was added to each. The crystallized salt components were analyzed through compositional testing.

### 2.5. Ethanol parameter optimization experiments

During the ethanol parameter optimization experiments, 50 mL of saturated ammonium sulfate waste salt solution was taken in a conical flask for each group, and 100 mL of ethanol was added respectively. First, the temperature influence exploration experiment was carried out. By using a low-temperature thermostatic bath to simulate the fluctuating industrial water temperature under extreme climatic conditions, the reaction environment temperature was controlled successively at 2 °C, 5 °C, 10 °C, 15 °C, 20 °C, 25 °C, 30 °C, 35 °C, 40 °C, and 50 °C. The

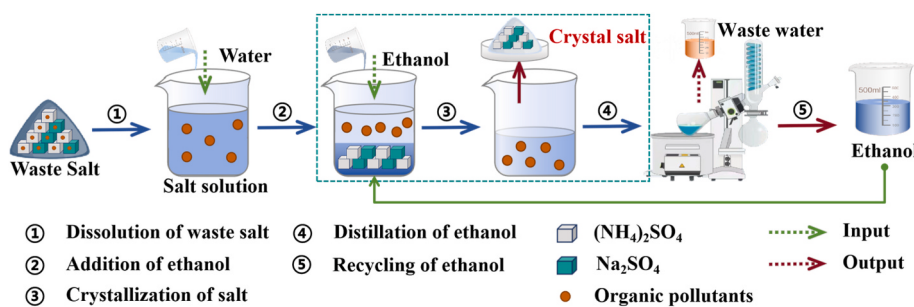


Fig. 1. Process for removing organic pollutants from ammonium sulfate waste salt and recovering crystalline salt.

mechanical stirring speed was kept at 500 r/min, and the reaction time was set at 120 min. Secondly, for the reaction time parameter optimization experiment, under the constant temperature condition of 25 °C, the reaction time was set at 15, 30, 45, 60, 120, and 240 min respectively, with other experimental conditions remaining unchanged. Finally, when optimizing the pH value parameter, the system pH value was adjusted from 2.0 to 8.0 using 0.1 M H<sub>2</sub>SO<sub>4</sub>/NaOH standard solution, which range ensured the stability of ammonium sulfate and no ammonia loss, and reactions were conducted at 25 °C for 120 min. After the above experiments were completed, the solutions obtained were filtered, the crystalline salt was collected and dried, and the yield of the product salt, TOC and other indicators were detected.

## 2.6. Ethanol recovery and reuse

Ethanol was recovered using a rotary evaporator with a temperature gradient set at 35–60 °C (increasing by 5 °C each step), a rotation speed of 120 rpm, and a vacuum pressure of –0.1 MPa. The process was stopped when the volume of the condensed solution reached the ethanol addition amount used in the previous process, and the stopping time was recorded. After each ethanol recovery, the purity of ethanol was determined by a gas chromatograph equipped with a flame ionization detector (FID), and then the next cycle experiment was performed. In the experiment to determine the optimal addition amount of recovered ethanol, 15 groups of 50 mL saturated ammonium sulfate waste salt solution were each mixed with 50–250 mL of recovered ethanol (increasing by 50 mL each step) at a temperature of 35 °C. The yield of the product salt and the TOC (Total Organic Carbon) were compared. To further investigate the recycling effect of recovered ethanol, 150 mL of recovered ethanol was added at a volume ratio of 3:1, and used in seven consecutive ASC process cycles (beyond which marked declines in ethanol purity and salt yield were observed). Ethanol purity and reuse efficacy were monitored and analyzed throughout each cycle.

## 2.7. Characterization methods

Anion concentrations in water (F<sup>−</sup>, NO<sub>3</sub><sup>−</sup>, NO<sub>2</sub><sup>−</sup>, Br<sup>−</sup>, Cl<sup>−</sup>, SO<sub>4</sub><sup>2−</sup>) were analyzed via ion chromatography (IC, ICS600, Thermo Fisher; limit of detection (LOD): 0.01 ppm). Cation contents in samples were measured by inductively coupled plasma optical emission spectrometry (ICP, Prodigy, Leeman; LOD: 0.01 ppm). Sample preparation involved weighing 0.1 g of the sample into a digestion canister, adding 2 mL HCl, 3 mL HF, and 1 mL H<sub>2</sub>O<sub>2</sub> (note: acid handling must be completed in a fume hood and wearing protective equipment). Digestion was carried out at 180 °C for 2.5 h. After cooling, the solution was diluted to 100 mL and then analyzed. Organic carbon in waste salt was determined using a total organic carbon analyzer (TOC-L, CHP, Shimadzu; LOD: 0.05 ppm). Ammonia nitrogen in samples was quantified with a double-beam UV–Vis spectrophotometer (TU-1900, Beijing Purkinje). The crystalline phases of samples were characterized by X-ray diffraction (XRD, PANalytical, Netherlands). The morphology and elemental composition of salt samples were investigated using a field-emission environmental scanning electron microscope (SEM, Quattro, USA) combined with energy-dispersive X-ray spectroscopy (EDS, EDAX).

## 3. Results and discussion

### 3.1. Antisolvent type screening

Different antisolvents were added to saturated (NH<sub>4</sub>)<sub>2</sub>SO<sub>4</sub>/Na<sub>2</sub>SO<sub>4</sub> solutions, significantly affecting salt crystallization. As shown in Fig. 2a, among eight antisolvents tested at a 3:1 vol ratio, methanol and ethanol showed excellent effects. Methanol achieved a 98.94 % Na<sub>2</sub>SO<sub>4</sub> crystallization yield and a 67.86 % (NH<sub>4</sub>)<sub>2</sub>SO<sub>4</sub> yield, while ethanol had a 95.73 % Na<sub>2</sub>SO<sub>4</sub> yield and a 70.88 % (NH<sub>4</sub>)<sub>2</sub>SO<sub>4</sub> yield. Acetonitrile, isopropanol, and acetone also demonstrated good crystallization ability. The results confirmed that specific antisolvents can effectively induce ion recrystallization in salt solutions. This phenomenon may be attributed to the molecular structure of the solvents, methanol, ethanol, and

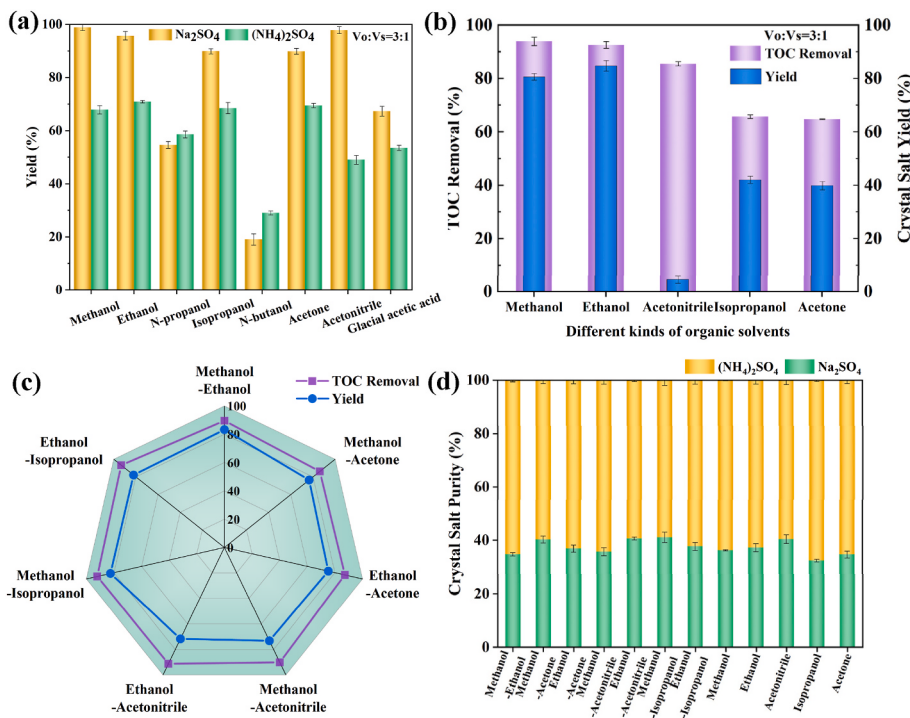


**Fig. 2.** Effect of antisolvent crystallization on ammonium sulfate waste salt treatment: (a) Crystallization yield of eight antisolvents in saturated (NH<sub>4</sub>)<sub>2</sub>SO<sub>4</sub>/Na<sub>2</sub>SO<sub>4</sub> solutions, (b) Organic pollutant removal and crystallization yield of antisolvents in actual waste salt solutions, (c) Comparison of binary solvent mixtures' synergistic treatment effects, (d) Component regulation of crystallized salt by different antisolvents.

isopropanol all possess hydroxyl groups that readily form hydrogen bonds with water molecules, thereby disrupting the solvation shells of salt ions and promoting crystal precipitation (Li et al., 2020b). Fig. 2b compared the organic pollutant removal efficiency of five antisolvents in ammonium sulfate waste salt. Ethanol showed the highest removal rate at 93.87 %, followed by methanol at 92.51 %. Acetonitrile, isopropanol, and acetone had lower efficiencies of 85.49 %, 65.71 %, and 64.73 %, respectively. This result was consistent with literature reports indicating that organic solutes are substantially more soluble in methanol and ethanol than that in other solvents such as isoacetone (Wanxin et al., 2018). Combined with the analysis of crystallization yield, methanol and ethanol achieved 84.7 % and 80.56 %, while the other three solvents remained below 43 %. Overall, methanol and ethanol were preferred for ammonium sulfate waste salt treatment due to their ability to maintain crystallization yields above 80 % and remove over 92 % of organic pollutants.

Given that methanol and ethanol had already demonstrated excellent performance in single-solvent systems, binary mixed systems (B–G groups) were constructed and tested to explore whether their combination with acetone, acetonitrile, or isopropanol could produce synergistic effects. As shown in Fig. 2c, these binary systems outperformed their corresponding single-solvent systems. Specifically, organic pollutant removal increased by 4.63–26.41 percentage points, and crystallization yield rose by 35.3–68.7 percentage points. However, none of the binary systems (A–G groups) surpassed the removal efficiencies of single-methanol (93.87 %) and single-ethanol (92.51 %) systems, with removal rates of 86.16–92.23 %. In crystallization, the highest-yielding binary system, methanol-ethanol, achieved 83.24 %, close to the single-methanol (80.56 %) and single-ethanol (84.7 %) values, indicating no superiority over single-solvent systems. Additionally, component purity analysis (Fig. 2d) revealed that salt-product compositions from binary mixtures had compositions almost identical to those from single solvents. In summary, binary systems underperformed compared to single-methanol and single-ethanol systems, so the latter were preferred for process optimization.

### 3.2. Comparison of methanol and ethanol performance

To assess the effect of antisolvent dosage on ammonium sulfate waste salt treatment, the experiment established a gradient of antisolvent-to-solution volume ratios ( $V_0:V_s$ ) within the commonly used range of 0–3 as reported in the literature (Huang et al., 2025). Fig. 3a and b illustrated the performance differences of methanol and ethanol at various volume ratios. The results indicated that when the antisolvent dosage was 100 mL, corresponding to a  $V_0:V_s$  ratio of 2:1, both methanol and ethanol achieved optimal performance. Specifically, ethanol demonstrated a high organic pollutant removal rate of 96.44 % and a salt crystallization yield of 85.07 %, while methanol showed an organic pollutant removal rate of 94.04 % and a salt crystallization yield of 79.62 %. These findings confirmed that a  $V_0:V_s$  ratio of approximately 2:1 was optimal, with ethanol outperforming methanol in both aspects. Further experiments within the  $V_0:V_s$  range of 2(±0.3):1 revealed that while the organic pollutant removal rate remained relatively stable, the salt crystallization yield peaked at a precise  $V_0:V_s$  ratio of 2:1. Thus, the optimal antisolvent dosage ratio was determined to be 2:1.

Fig. 3c revealed that in the mixed salt system, ethanol's crystallization yield was consistently higher than that of methanol, remaining above 80 % when the  $(\text{NH}_4)_2\text{SO}_4$  to  $\text{Na}_2\text{SO}_4$  ratio ranged from 0.25 to 4 (corresponding to  $(\text{NH}_4)_2\text{SO}_4$  purity of 20 %–80 %). However, the crystallization yield decreased as the proportion of  $(\text{NH}_4)_2\text{SO}_4$  in the solution increased. Fig. 3d further analyzed the purity of the crystallized salt obtained at different mixed salt ratios. Results showed that the purity of  $\text{Na}_2\text{SO}_4$  in the crystallized salt was significantly higher than that in the mixed salt solution. Specifically, the  $\text{Na}_2\text{SO}_4$  purity in the salt crystals obtained from ethanol increased by 9.69–21.02 %, while that from methanol increased by 14.53–29.53 %. When the  $\text{Na}_2\text{SO}_4$  purity in the mixed salt solution was 80 %, the  $\text{Na}_2\text{SO}_4$  purity in the salt crystals from ethanol reached 97.65 %, compared to 99.42 % from methanol. This may be because  $(\text{NH}_4)_2\text{SO}_4$  is more soluble than  $\text{Na}_2\text{SO}_4$  in the antisolvent-water mixture, making it harder for  $(\text{NH}_4)_2\text{SO}_4$  to lose its hydration shell and crystallize (Li et al., 2021), thereby resulting in

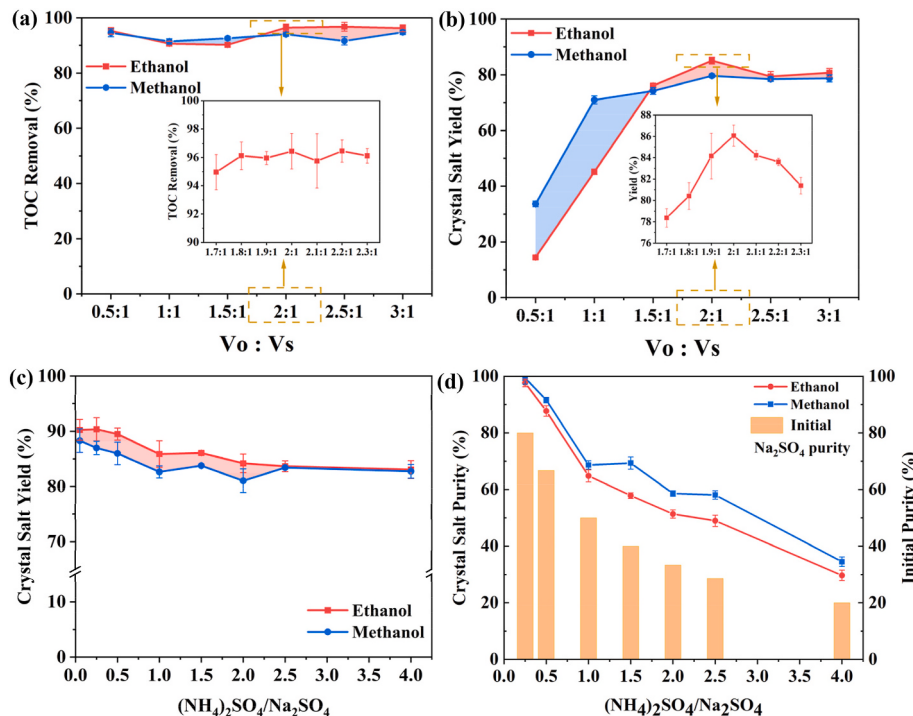


**Fig. 3.** Properties of methanol and ethanol in saturated ammonium sulfate waste salt solutions: (a) Organic pollutant removal at different dosages, (b) Crystallization yield of salt crystals at different dosages, (c) Crystallization yield of salt from solutions of varying purity, (d) Purity of crystallized salt from solutions of varying purity.

relatively higher  $\text{Na}_2\text{SO}_4$  content in the salt crystals. Considering the overall performance of methanol and ethanol, ethanol was selected as the antisolvent for ammonium sulfate waste salt treatment, with an optimal volume ratio of 2:1 between the antisolvent and salt solution.

### 3.3. Optimization of ethanol operation conditions

The influence of temperature, reaction time, and pH on the performance of ethanol in treating ammonium sulfate waste salt solutions was systematically evaluated. Fig. 4a showed that temperature significantly affected ethanol treatment of ammonium sulfate waste salt solutions. Between 0 and 15 °C, the salt crystallization yield positively correlated with temperature, averaging 91.34 %. However, when the temperature exceeded 15 °C, the yield gradually decreased, reaching 78.93 % at 30 °C and further dropping to 66.61 % at 50 °C. This phenomenon is attributed to the elevated temperature increasing  $\text{Na}_2\text{SO}_4$  solubility in the solution (Wang et al., 2020), while simultaneously weakening hydrogen-bond interactions between ethanol and water molecules (Liu et al., 2025), thereby reducing solution supersaturation and diminishing the driving force for crystal nucleation (Yang et al., 2022). The organic pollutant removal rate remained stable at 95.97 % between 0 and 30 °C but decreased markedly to 75.6 % at 50 °C. Considering both performance indicators, the TOC removal rate remained excellent (>95 %) throughout the 0–30 °C range, and the crystallization yield at 30 °C still in the conventional range of waste salt resource recovery rate (~80 %) (Huang et al., 2024). Therefore, 0–30 °C was determined as the optimal temperature operation range of ASC process.

Fig. 4b explored how reaction time affected ethanol's pollutant removal and salt crystallization. The best results occurred at 1 h reaction time, with a 97.46 % removal rate and an 84.43 % salt yield. This indicated that ethanol could efficiently remove pollutants and promote salt crystallization within a short time. Fig. 4c demonstrated that within a pH range of 2–8, there was no significant impact on ethanol's pollutant removal efficiency or salt crystallization. Thus, pH adjustment was unnecessary for industrial applications.

To assess the statistical significance of the experimental results, Pearson correlations between temperature, reaction time, and pH versus TOC removal and crystal yield were analyzed (Table S2). The Pearson correlation coefficient ( $r$ ) quantifies the strength of the linear relationship, with larger absolute values indicating stronger associations (Zhang et al., 2023). Temperature exhibited significant negative correlations with both TOC removal ( $r = -0.747$ ,  $p < 0.05$ ) and crystal yield ( $r = -0.951$ ,  $p < 0.01$ ), indicating that the increase of temperature will reduce the process performance. Although pH was positively correlated with TOC removal ( $r = 0.830$ ,  $p < 0.05$ ) and crystal yield ( $r = 0.956$ ,  $p < 0.01$ ), the improvement observed in actual operation was small. Reaction time showed weak correlations with the two response variables ( $r = 0.083$  and  $-0.397$ ), indicating its influence was negligible. Overall, temperature exerted the greatest impact on ethanol treatment efficiency, whereas reaction time and pH played minor roles.

### 3.4. Ethanol recovery conditions and Usage effects

To determine the optimal ethanol recovery conditions, distillation experiments were conducted on filtrate components under various temperatures and times. Fig. 5a illustrated the recovery efficiency of ethanol at different temperatures. The experiments were designed to achieve 100 % ethanol recovery. Results indicated that low-temperature recovery yielded the highest ethanol purity, which decreased significantly as the temperature increased. At a recovery temperature of 35 °C, the process took the longest time of 1.35 h. Conversely, at 60 °C, the recovery time was markedly reduced to 15 min, indicating that higher temperatures accelerated the ethanol recovery rate. To maintain high ethanol purity, 35 °C was chosen as the recovery temperature. Fig. 5b showed the ethanol recovery rate at 35 °C. The recovery rate increased significantly with time, reaching 98.39 % at 105 min, which is close to the theoretical efficiency.

To investigate the recycling efficiency of recovered ethanol, experiments were conducted to evaluate its impact on organic pollutant removal and salt crystallization yield under different conditions. Fig. 5c showed that increasing the dosage of recovered ethanol stabilized the organic pollutant removal rate at an average of 93.91 %, while the salt crystallization yield increased. The inflection point occurred at a recovered ethanol to waste salt solution ratio of 2:1, where the salt yield reached 75.32 %. At a ratio of 3:1, the removal rate was 93.41 %, and the salt yield slightly increased to 78.22 %. Considering the potential performance degradation of ethanol after recycling (e.g., decreased purity and impurities accumulation), increasing the dosage ratio (Vo:Vs = 3:1) can compensate for the efficiency loss. From the perspective of long-term operational stability, a ratio of 3:1 was finally selected as the optimal ratio.

Fig. 5d further examined the effect of multiple ethanol recovery cycles on ammonium sulfate waste salt treatment. Results showed that between 1 and 7 recovery cycles, the organic pollutant removal rate remained approximately 93.99 %, but the salt crystallization yield significantly decreased with more cycles, dropping to 70.27 % after seven cycles. Additionally, the purity of recovered ethanol decreased markedly with each cycle, reaching 55.51 % after the seventh cycle. This indicates that while ethanol remains effective in removing organics after multiple uses, both the salt yield and ethanol purity gradually decrease with increasing recovery cycles. The salt yield declined because water accumulated and trace low-boiling organics enriched during ethanol recovery, which alter the physicochemical properties of ethanol and consequently inhibit nucleation and growth in the ASC process.

### 3.5. Comparison of different TOC removal methods

Pyrolysis and advanced oxidation are common methods for removing organic pollutants. Fig. 6a showed that as the pyrolysis temperature increased, both the organic pollutant removal rate and ammonia nitrogen loss increased. At 350 °C, the maximum organic removal rate of 87.43 % was achieved, but ammonia nitrogen loss also peaked at 57.32 %. Notably, higher temperatures also increase ammonia

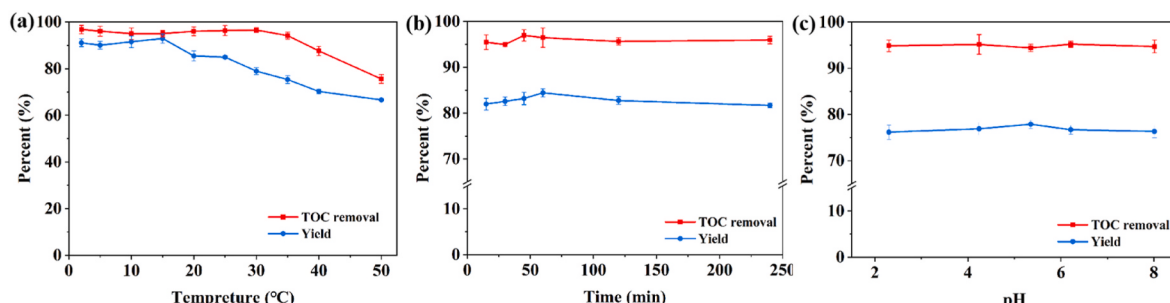
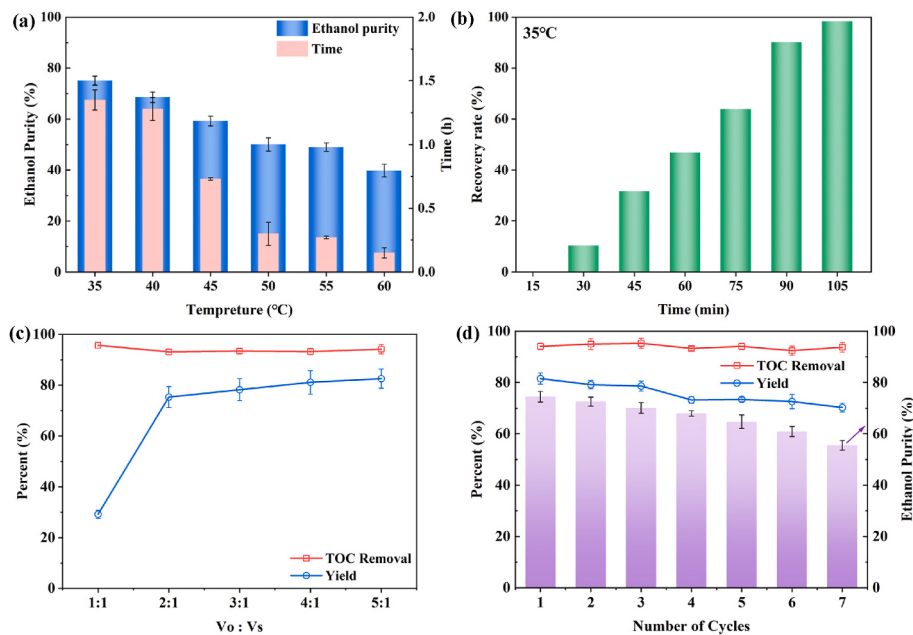
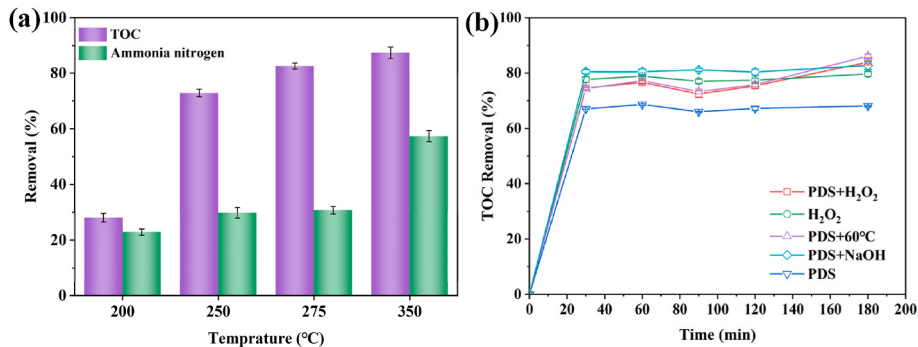


Fig. 4. Effect of ethanol treatment on ammonium sulfate waste salt under different conditions: (a) temperature, (b) time, (c) pH.



**Fig. 5.** Ethanol recovery conditions and reuse effects: (a) Impact of temperature and time on ethanol recovery purity, (b) Effect of time on ethanol recovery rate, (c) Treatment of waste salt with recovered ethanol, (d) Reuse effects of ethanol over multiple cycles.



**Fig. 6.** Methods for removing organic pollutants from ammonium sulfate waste salt: (a) pyrolysis, (b) advanced oxidation.

gas production, which may corrode equipment.

Fig. 6b demonstrated the effectiveness of advanced oxidation in degrading organic pollutants in ammonium sulfate waste salt. Using PDS activated by NaOH, H<sub>2</sub>O<sub>2</sub>, or heat (60 °C) generated oxidative free radicals (e.g., ·SO<sub>4</sub><sup>-</sup>, ·OH). After 180 min, the TOC removal rate was 68.12 % with only PDS, 82.70 % with NaOH activated PDS, 83.94 % with H<sub>2</sub>O<sub>2</sub> activated PDS, and 86.17 % with heat activated PDS.

Overall, the ASC method showed significant advantages over pyrolysis and advanced oxidation in removing organic pollutants from ammonium sulfate waste salt. At room temperature, it achieved over 95 % organic pollutant removal, which was 7.57 and 8.83 percentage points higher than the best case scenarios for pyrolysis at 350 °C and heat-activated advanced oxidation, respectively. More importantly, antisolvent crystallization also offered stable salt recovery of over 80 % and avoided secondary pollution.

### 3.6. Economic and environmental cost analysis

According to the experimental results of ASC process, the economic evaluation was carried out. The treatment of 1 ton of ammonia sulfate waste salt required 3.8 tons of ethanol. Assuming that the process is continuous and the ethanol was recycled, the ethanol loss rate is 5 %. As shown in Table S3, the total process cost amounted to 1350 CNY, of

which ethanol accounted for the dominant share (1140 CNY). Notably, process optimization that reduced the ethanol loss rate to 1 % would cut this cost to only 228 CNY. Compared with other ASC waste salt treatments, the economic difference mainly depended on the dosage and loss rate of antisolvent. For example, the acetone process required 10 tons of acetone per ton of pyridine-containing waste salt (loss rate of 2.5 %), giving a solvent cost of 1250 CNY and a total cost of 1376 CNY (Li et al., 2020a). In contrast, the ethanol process treating a mixed sodium chloride and sodium sulfate waste salt used 5 tons of ethanol (loss rate of 1 %), resulting in an ethanol cost of 350 CNY and a total cost of 476 CNY (Wang et al., 2024a). Thus, the economics of the antisolvent in industrial applications largely depended on its dosage and the control of recovery losses. Overall, compared to processes such as pyrolysis (500–1000 CNY/t) and high-temperature melting (1600–3000 CNY/t) (Feng et al., 2025), the ASC process demonstrated certain competitiveness in terms of cost.

The whole life cycle assessment (LCA) of the process was carried out by Gabi 10.0 software, and the life cycle list is shown in Table S4. The ethanol in the model was derived from the biomass fermentation process, and the power emission factor was 0.568 kg CO<sub>2</sub>/kWh. LCA results (Table S5) showed that the global warming potential (GWP) of 1 ton of ammonium sulfate waste salt was 304 kg CO<sub>2</sub> eq., which was significantly lower than that of traditional methods such as pyrolysis of sodium

chloride-based waste salt (1144 kg CO<sub>2</sub> eq (Huang et al., 2024)) and ASC treatment of sodium chloride and sodium sulfate mixed waste salt (848–2401 kg CO<sub>2</sub> eq (Sahu et al., 2024; Huang et al., 2025)). This is mainly due to the fact that ethanol itself is a clean energy, and the recovery and recycling of ethanol are realized in the process, which greatly reduces the carbon emissions in the production process.

### 3.7. Characterization of crystallized salt

XRD was used to analyze the crystalline composition of the product salt. As shown in Fig. 7a, the diffraction peaks of the product salt obtained via antisolvent crystallization matched the characteristic peaks of ammonium sulfate (standard card PDF#00-040-0660) and sodium sulfate (standard card PDF#70-1541), confirming that the product salt mainly consisted of ammonium sulfate and sodium sulfate. To quantify the differences in crystal structure, the relative crystallinity of the material was calculated (Nomura et al., 2020). The integrated intensity of the crystalline phase diffraction peaks was calculated as 2602, and the total integrated intensity of all diffraction (including crystalline peaks and amorphous scattering) was 3263, based on the diffraction data within the 20 = 5–60° range. The relative crystallinity of the sample was thus determined to be 80 %. This result indicates a well-crystallized product.

SEM was employed to observe the morphological changes of crystals in ammonium sulfate waste salt before and after organic pollutant removal. As shown in Fig. 7b, the original salt crystals exhibited irregular geometry, uneven crystal face development, and a rough surface, accompanied by a large number of disordered stacking structures, which may be attributed to interference from organic impurities and inconsistent crystallization conditions. After pyrolysis treatment (Fig. 7c), the crystals displayed a smoother surface and a distinct layered structure, highly consistent with the typical microstructure of sodium sulfate. This observation indicates that the pyrolysis process effectively removed

organic pollutants coated on the crystal surface, while also decomposing ammonium sulfate and facilitating its transformation into the sodium sulfate crystal form. In contrast, the sample treated with antisolvent crystallization (Fig. 7d) exhibited significantly different morphological features, showing orderly stacked crystals with a regular structure and clear three-dimensional morphology. This morphological transformation confirms that the antisolvent crystallization method effectively promotes uniform nucleation and directional crystal growth by controlling the crystallization kinetics, thereby achieving structural reorganization of the crystals.

Fig. 7e–g presents the elemental mapping images of the original ammonium sulfate waste salt, pyrolysis-treated salt, and ASC salt. The results showed a significant reduction in carbon content before and after organic pollutant removal. Specifically, the carbon content in the original salt was 31.7 % (Fig. 7h), decreased to 18 % after pyrolysis (Fig. 7i). This trend was consistent with the results measured by the TOC analyzer (original salt: 7149.54 mg/kg; pyrolysis salt: 1242.26 mg/kg), indicating that high temperatures caused organic components to fracture, pyrolyze, and vaporize, leading to the destruction and removal of organic carbon structures. Notably, in the ASC salt, the carbon content was only 0.3 % (Fig. 7j), and the corresponding TOC analyzer content was 227.21 mg/kg, demonstrating the high efficiency of the ASC process in removing organic pollutants. The discrepancy in carbon content characterization between EDS and TOC was due to the fact that organic pollutants tend to accumulate on the surface of salt particles. Since EDS only quantified elements on the sample surface, it yielded relatively higher carbon content values, while TOC reflected the total organic carbon content in the bulk phase of the sample.

### 3.8. Reaction mechanism

The schematic diagram of the reaction mechanism of antisolvent crystallization for organic pollutant removal is shown in Fig. 8. The

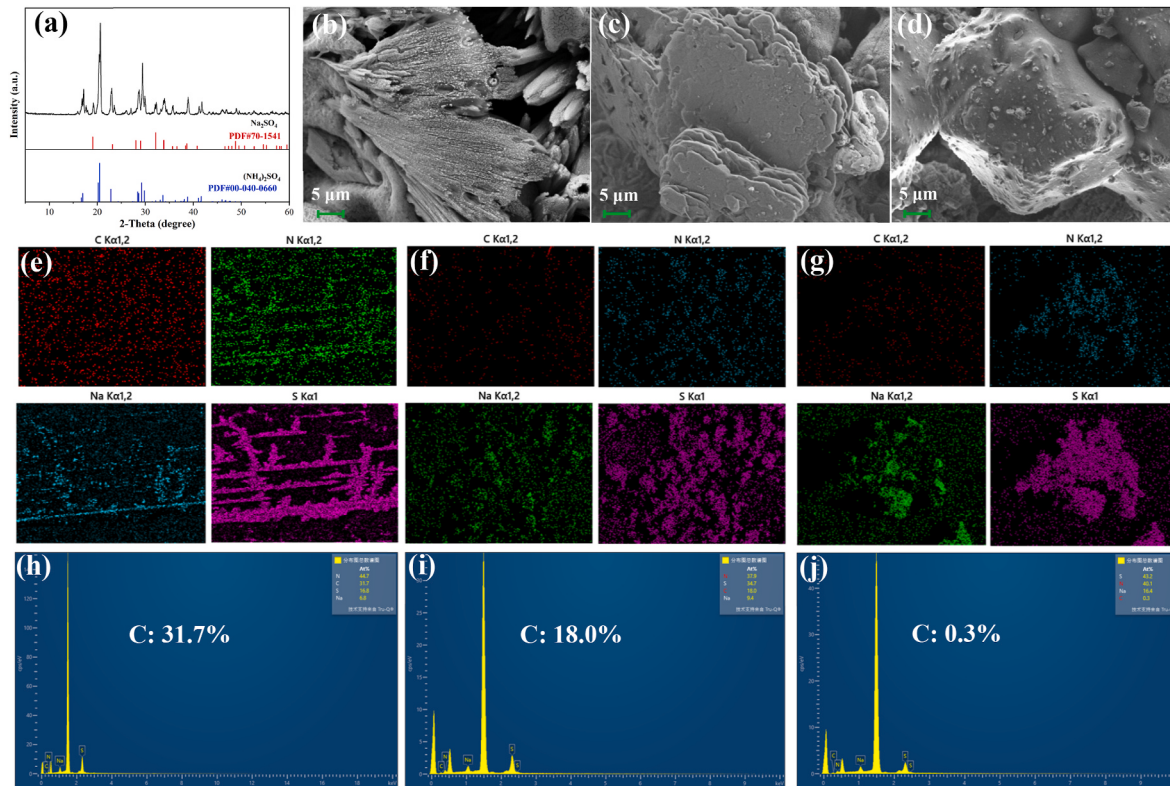


**Fig. 7.** Characterization of waste salt and crystallized salt: (a) XRD pattern of crystallized salt; SEM images of (b) original salt, (c) pyrolysis salt, and (d) antisolvent-crystallized salt; elemental mappings of (e) waste salt, (f) pyrolysis salt, and (g) solvent-crystallized salt; EDS images of (h) waste salt, (i) pyrolysis salt, and (j) solvent-crystallized salt.

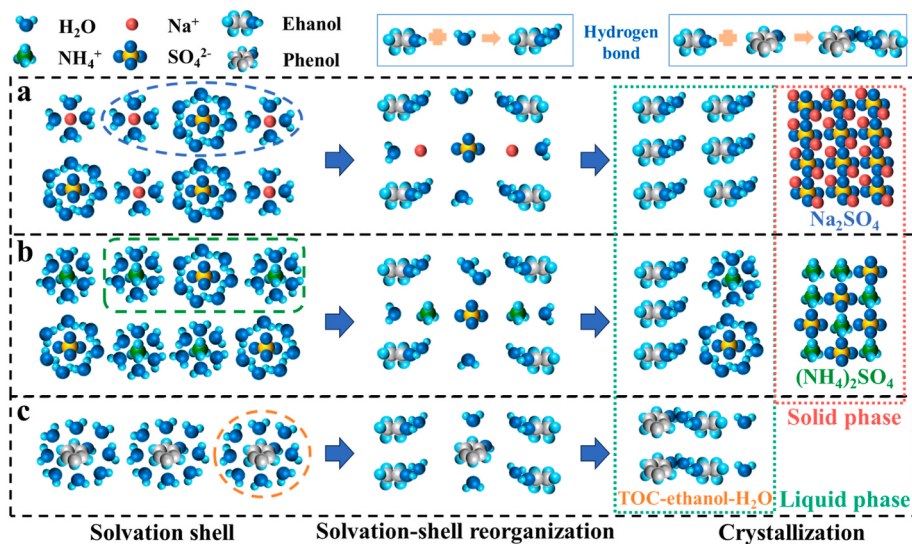


Fig. 8. Schematic of the reaction mechanism for organic pollutant removal.

process can be divided into three steps. Initially, when the waste salt crystals were dissolved in an aqueous solution, the salt crystal structure dissociated into ionic states, and the organic substances were concomitantly released into the salt solution. At this point, the salt ions and organic molecules in the solution were enveloped by solvation shell (Dighe and Singh, 2019). Subsequently, upon the introduction of a specific antisolvent, such as ethanol, into the saturated waste salt solution, the antisolvent formed hydrogen bonds with water molecules, thereby disrupting the solvation shell of the salt ions and organic pollutants (Dette et al., 2010). Finally, the salt ions, stripped of their solvation shell, underwent a "clustering" phenomenon and re-aggregated into crystalline salts (Piana et al., 2006). In contrast, the organic pollutants primarily interacted with the antisolvent by hydrogen bonding and remained in the salt solution.

As shown in Fig. 8a and b, the crystallization of ammonium sulfate and sodium sulfate involved the dissociation of  $\text{Na}^+$ ,  $\text{NH}_4^+$ , and  $\text{SO}_4^{2-}$  ions, which were initially surrounded by solvation shell. When ethanol was introduced into the solution, it caused the salt ions to lose their solvation shell, leading to the formation of a mixed crystal of  $\text{Na}_2\text{SO}_4$  and  $(\text{NH}_4)_2\text{SO}_4$ . It was important to note that some  $(\text{NH}_4)_2\text{SO}_4$  remained in the solution. This is consistent with previous findings that  $(\text{NH}_4)_2\text{SO}_4$  has a higher solubility than  $\text{Na}_2\text{SO}_4$  in the  $\text{H}_2\text{O}$ -monoethanolamine antisolvent system (Li et al., 2021). Fig. 8c illustrated the removal of organic pollutants, using phenol as a representative example (Liu et al., 2024; Xu et al., 2025). Phenol, originally surrounded by a solvation shell in the solution, lost this shell upon ethanol addition and became dissolved in the ethanol-water solution. Researchers have employed molecular dynamics simulations to calculate changes in coordination numbers, local density differences, and instantaneous water coverage around the solute molecules, confirmed at the molecular level that ethanol gradually replaces water and triggered the collapse of the solvation shell (Dighe et al., 2022; Xue et al., 2021). The organic pollutants were remained in the solution, while the salt crystals reformed through re-crystallization, achieving effective separation.

#### 4. Conclusions

This study developed an efficient ASC process for the treatment of ammonium sulfate waste salt. The process operates efficiently under conventional operating conditions (0–30 °C, pH = 2–8), achieving an organic pollutant removal rate of 96.44 % and a salt recovery rate of 85.07, demonstrating strong potential for industrial application. Ethanol as the antisolvent can be recycled more than seven times while

maintaining stable treatment performance, significantly reducing raw material consumption and operating costs. Compared to pyrolysis and advanced oxidation processes, ASC shows better comprehensive performance in terms of pollutant removal and salt recovery. Mechanistic studies revealed that the addition of ethanol effectively disrupts the solvation structure of salt ions, thereby inducing crystallization and enabling efficient pollutant separation. However, the industrial scaling of this technology still faces several engineering challenges, including crystallizer design, crystallization kinetics regulation, ethanol distillation purity and loss control, as well as waste liquid treatment. Subsequent research will focus on pilot scale test, emphasizing the evaluation of scale-up effects, long-term operational stability, and full-process technical economy, so as to promote the industrial adoption of this technology.

#### CRediT authorship contribution statement

**Xinyu Huang:** Writing – original draft, Conceptualization. **Hao Wang:** Methodology, Data curation. **Saijun Lv:** Project administration. **Haoqing Zhang:** Software. **Chuqi Wang:** Validation. **Xiuxiu Ruan:** Writing – review & editing, Funding acquisition.

#### Declaration of competing interest

The authors declare that they have no known competing financial interests or personal relationships that could have appeared to influence the work reported in this paper.

#### Acknowledgements

This work was supported by the Science and Technology Commission of Shanghai Municipality (No. 22002400500); the National Nature Science Foundation of China (No. 20907029, No. 21577085). The authors gratefully acknowledge the financial support and cooperation work from Shaoxing Shangyu Zhonglian Environmental Protection Co., Ltd.

#### Appendix A. Supplementary data

Supplementary data to this article can be found online at <https://doi.org/10.1016/j.jclepro.2025.146751>.

## Data availability

Data will be made available on request.

## References

- Ahmad, N.N.R., Ang, W.L., Leo, C.P., et al., 2021. Current advances in membrane technologies for saline wastewater treatment: a comprehensive review. *Desalination* 517, 115170.
- Annamalai, S., Chandrasekaran, K., Shin, W.S., et al., 2022. Beyond dumping: new strategies in the separation of preservative salt from tannery waste mixed salt and its reuse for tannery industrial application. *Environ. Res.* 214, 113885.
- Bhatti, S., Sahu, P., Masani, H.R., et al., 2024. Process integration and techno-economic assessment of crystallization techniques for Na<sub>2</sub>SO<sub>4</sub> and NaCl recovery from saline effluents. *Chemical Engineering and Processing - Process Intensification* 203, 109879.
- Curić, I., Dolar, D., Karadakić, K., 2021. Textile wastewater reusability in knitted fabric washing process using UF membrane technology. *J. Clean. Prod.* 299, 126899.
- Dette, S.S., Stelzer, T., Jones, M.J., et al., 2010. Dehydration behaviour of hydrates. *Cryst. Res. Technol.* 45 (7), 697–702.
- Dighe, A.V., Singh, M.R., 2019. Solvent fluctuations in the solvation shell determine the activation barrier for crystal growth rates. *Proc. Natl. Acad. Sci.* 116 (48), 23954–23959.
- Dighe, A.V., Podupu, P.K.R., Coliaie, P., et al., 2022. Three-step mechanism of antisolvent crystallization. *Cryst. Growth Des.* 22 (5), 3119–3127.
- Domingues, E., Silva, M.J., Vaz, T., et al., 2022. Sulfate radical based advanced oxidation processes for agro-industrial effluents treatment: a comparative review with Fenton's peroxidation. *Sci. Total Environ.* 832, 155029.
- Dong, Z.J., Tao, Y.B., Ye, H., et al., 2024. Experimental and numerical study on pyrolysis characteristics of organic impurities in waste salt. *J. Clean. Prod.* 444, 141223.
- Du, S., Zhao, P., Wang, L., et al., 2023. Progresses of advanced anti-fouling membrane and membrane processes for high salinity wastewater treatment. *Results Eng.* 17, 100995.
- Feng, L., Tian, B., Chen, L., et al., 2024. Purification and recovery of NaCl from epoxy resin waste salt through an integrated process based on aqueous two-phase systems (ATPS). *J. Environ. Chem. Eng.* 12 (3), 113091.
- Feng, L., Tian, B., Zhu, M., et al., 2025. Current progresses in the analysis, treatment and resource utilization of industrial waste salt in China: a comprehensive review. *Resour. Conserv. Recycl.* 217, 108224.
- Gholami, A., Mousavi, S.B., Heris, S.Z., et al., 2024. Highly efficient treatment of petrochemical spent caustic effluent via electro-Fenton process for COD and TOC removal: optimization and experimental. *Biomass Conversion and Biorefinery* 14 (15), 17481–17497.
- Goh, P.S., Wong, K.C., Ismail, A.F., 2022. Membrane technology: a versatile tool for saline wastewater treatment and resource recovery. *Desalination* 521, 115377.
- Huang, X., Wang, H., Song, M., et al., 2024. Comparative organic pollutants removal efficiency and life cycle assessment of pyrolysis and solvent elution for industrial waste salt recycling. *J. Environ. Manag.* 371, 123218.
- Huang, X., Song, M., Wang, H., et al., 2025. Waste salt separation by antisolvent crystallization process: mechanism study of Na<sub>2</sub>SO<sub>4</sub>-NaCl-solvent ternary phase diagrams and its life cycle assessment. *Desalination* 613, 118985.
- Li, J., Zheng, J., Peng, X., et al., 2020a. NaCl recovery from organic pollutants-containing salt waste via dual effects of aqueous two-phase systems (ATPS) and crystal regulation with acetone. *J. Clean. Prod.* 260, 121044.
- Li, X., He, Y., Xu, Y., et al., 2020b. 5-Nitrosalicylaldehyde in aqueous co-solvent mixtures of methanol, ethanol, isopropanol and acetonitrile: solubility determination, solvent effect and preferential solvation analysis. *J. Chem. Therm.* 142, 106014.
- Li, B., Zhang, X., Li, Z., 2021. Phase diagram for the Na<sub>2</sub>SO<sub>4</sub>-(NH<sub>4</sub>)<sub>2</sub>SO<sub>4</sub>-MEA-H<sub>2</sub>O system at elevated temperature. *J. Chem. Eng. Data* 66 (8), 3012–3019.
- Li, C., Xu, X., Liu, M., et al., 2024. Treatment of high-salinity organic wastewater by advanced oxidation processes: research progress and prospect. *J. Water Proc. Eng.* 60, 105272.
- Lin, C., Chi, Y., Jin, Y., et al., 2018. Molten salt oxidation of organic hazardous waste with high salt content. *Waste Manag. Res.* 36 (2), 140–148.
- Liu, H., Xu, T., Li, C., et al., 2021. High increase in biodegradability of coking wastewater enhanced by Mn ore tailings in Fenton/O<sub>3</sub> combined processes. *Int. J. Environ. Sci. Technol.* 18 (1), 173–184.
- Liu, Y., Sun, Y., Li, Y., et al., 2024. A closed-loop integrated process of bipolar membrane electrodialysis and resin adsorption for resource recovery from high-salinity phenolic wastewaters: salicylic acid manufacturing wastewater as a representative. *Chem. Eng. J.* 482, 148681.
- Liu, J., Pearlstein, A.J., Feng, H., 2025. Effects of operating parameters on single-stage ultrasonic separation of ethanol from its aqueous solutions. *Sep. Purif. Technol.* 353, 128179.
- Lo, C., Wijffels, R.H., Eppink, M.H.M., 2024. Lipid recovery from deep eutectic solvents by polar antisolvents. *Food Bioprod. Process.* 143, 21–27.
- Lu, Q., Kou, Y., Xiao, L., et al., 2025. Breaking the energetic ammonium salts decomposition barrier: atomically dispersed Fe catalysts unveil the pyrolysis mechanisms and oxygen release strategies. *J. Catal.* 451, 116357.
- Ni, S., Wu, C., Wang, Y., et al., 2019. An extraction and precipitation process for the removal of Ca and Mg from ammonium sulfate rare Earth wastewaters. *Hydrometallurgy* 187, 63–70.
- Nomura, S., Kugo, Y., Erata, T., 2020. <sup>13</sup>C NMR and XRD studies on the enhancement of cellulose II crystallinity with low concentration NaOH post-treatments. *Cellulose* 27 (7), 3553–3563.
- Piana, S., Jones, F., Gale, J.D., 2006. Assisted desolvation as a key kinetic step for crystal growth. *J. Am. Chem. Soc.* 128 (41), 13568–13574.
- Qiu, J., Albrecht, J., Janev, J., 2020. Solubility behaviors and correlations of common solvent-antisolvent systems. *Org. Process Res. Dev.* 24 (11), 2722–2727.
- Raluy, G., Serra, L., Uche, J., 2006. Life cycle assessment of MSF, MED and RO desalination technologies. *Energy* 31 (13), 2361–2372.
- Ruan, X., Song, M., Fang, Z., et al., 2024. Methods to treat industrial salted waste: a review. *Environ. Chem. Lett.* 22 (4), 2035–2053.
- Sahu, P., Gao, B., Bhatti, S., et al., 2024. Process design framework for inorganic salt recovery using antisolvent crystallization (ASC). *ACS Sustain. Chem. Eng.* 12 (1), 154–165.
- Sussens, J., Chivavava, J., Lewis, A.E., 2024. The recovery of yttrium sulfate through antisolvent crystallization using alcohols. *Sep. Purif. Technol.* 346, 127459.
- Wang, L., Yang, H., Si, Z., et al., 2020. Solubility and thermodynamics of d-glucosamine 2-sulfate sodium salt in water and binary solvent mixtures with methanol, ethanol and n-propanol. *J. Mol. Liq.* 300, 112218.
- Wang, X., Gong, Y., Qin, J., et al., 2021. Deep removal of organic matter in glyphosate contained industrial waste salt by dielectric barrier discharge plasma. *J. Environ. Chem. Eng.* 9 (5), 106295.
- Wang, X., Li, Y., Gong, Y., et al., 2023. Deep purification of industrial waste salt containing organic pollutants by a dry method with non-thermal plasma. *Sep. Purif. Technol.* 308, 122904.
- Wang, J., Hong, X., Fang, G., et al., 2024a. Deep purification of pesticide waste salt containing high-concentration organic pollutants by ethanol solvents washing and heating treatment. *J. Environ. Chem. Eng.* 12 (3), 112480.
- Wang, S., Liu, H., Wu, Q., et al., 2024b. Catalytic janus nanoparticle-based recyclable emulsifiers for collaborative treatment of water-soluble and water-insoluble organic pollutants. *ACS Appl. Nano Mater.* 7 (12), 14820–14828.
- Wanxin, L., Li, M., Wang, N., et al., 2018. Solubility determination and modeling for 4-Nitrobenzonitrile in binary solvent mixtures of ethyl acetate plus (methanol, ethanol, n-Propanol, and isopropanol). *J. Chem. Eng. Data* 63 (10), 3933–3940.
- Xi, S., Wei, X., Ding, J., et al., 2023. The removal of organic contaminants from industrial waste salts by pyrolysis and potential use for energy storage. *J. Clean. Prod.* 425, 138931.
- Xu, G.-W., Shen, Y.-H., Shan, Y.-L., et al., 2025. Low-cost and sustainable fabrication of waste rubber derived porous carbon for o-nitrophenol removal with high practical application potential: a waste salt-free and recyclable template strategy. *Sep. Purif. Technol.* 354, 128901.
- Xue, S., Xu, J., Han, Y., et al., 2021. Solvent-antisolvent competitive interactions mediate imidacloprid polymorphs in antisolvent crystallization. *Cryst. Growth Des.* 21 (8), 4318–4328.
- Yaashikaa, P.R., Kumar, P.S., Nhung, T.C., et al., 2022. A review on landfill system for municipal solid wastes: insight into leachate, gas emissions, environmental and economic analysis. *Chemosphere* 309, 136627.
- Yang, H., Wang, H., Zhang, J., et al., 2019. A facile way to improve the performance of perovskite solar cells with toluene and diethyl ether mixed anti-solvent engineering. *Coatings* 9 (11), 766.
- Yang, L., Zhang, Y., Liu, P., et al., 2022. Kinetics and population balance modeling of antisolvent crystallization of polymorphic indomethacin. *Chem. Eng. J.* 428, 132591.
- Zelenková, G., Slovák, V., 2022. Decomposition of ammonium salts by quantitative TG-MS. *J. Therm. Anal. Calorim.* 147 (24), 15059–15068.
- Zhang, L., Fu, G., Zhang, Z., 2019. High-efficiency salt, sulfate and nitrogen removal and microbial community in biocathode microbial desalination cell for mustard tuber wastewater treatment. *Bioresour. Technol.* 289, 121630.
- Zhang, D., Li, C., Hao, Z., et al., 2021. Treatment performance and microbial community under ammonium sulphate wastewater in a sulphate reducing ammonium oxidation process. *Environ. Technol.* 42 (19), 2982–2990.
- Zhang, M., Li, W., Zhang, L., et al., 2023. A pearson correlation-based adaptive variable grouping method for large-scale multi-objective optimization. *Inf. Sci.* 639, 118737.
- Zhao, X., Zhang, S., Ma, H., et al., 2023. Feasibility study on A novel waste heat recovery process of industrial waste salt based on high temperature melting dry method. *E3S Web of Conferences* 385 (000), 4.